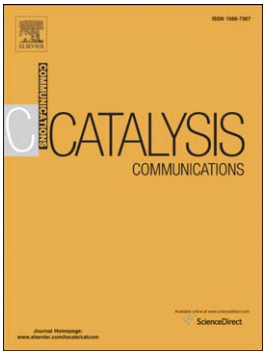

Production of renewable *p*-xylene from 2,5-dimethylfuran via Diels-Alder cycloaddition and dehydrative aromatization reactions over silica alumina aerogel catalysts

Yanuar Philip Wijaya, Dong Jin Suh, Jungho Jae

PII: S1566-7367(15)30017-0
DOI: doi: 10.1016/j.catcom.2015.07.008
Reference: CATCOM 4380

To appear in: *Catalysis Communications*

Received date: 18 May 2015
Revised date: 9 July 2015
Accepted date: 11 July 2015

Please cite this article as: Yanuar Philip Wijaya, Dong Jin Suh, Jungho Jae, Production of renewable *p*-xylene from 2,5-dimethylfuran via Diels-Alder cycloaddition and dehydrative aromatization reactions over silica alumina aerogel catalysts, *Catalysis Communications* (2015), doi: 10.1016/j.catcom.2015.07.008

Production of renewable *p*-xylene from 2,5-dimethylfuran via Diels-Alder cycloaddition and dehydrative aromatization reactions over silica alumina aerogel catalysts

Yanuar Philip Wijaya[1], Dong Jin Suh[1,2], Jungho Jae[1,2,*]

[1] *Clean Energy Research Center, Korea Institute of Science and Technology, Hwarang-ro 14-gil 5, Seongbuk-gu, Seoul 136-791, Republic of Korea;*
[2] *Department of Clean Energy and Chemical Engineering, Korea University of Science and Technology, 217 Gajeong-ro, Yuseong-gu, Daejeon 305-333, Republic of Korea.*
*jjae@kist.re.kr

Abstract

We report the selective conversion of biomass-derived 2,5-dimethylfuran (DMF) to *p*-xylene (~70% selectivity) through Diels-Alder cycloaddition and subsequent dehydration with silica alumina aerogel (SAA) catalysts. The high activity of SAA can be attributed to its high surface area, large mesoporous volume, and high acid site concentrations. The conversion of DMF and the yield of *p*-xylene were strongly dependent on the silica alumina ratio of SAA. A higher aluminum content in SAA led to a progressive increase in the concentration of Brønsted acid sites and a corresponding increase in the *p*-xylene production rate. The effect of solvent on the production of *p*-xylene was examined, and it was found that the *p*-xylene production rate increases significantly in polar aprotic solvents (i.e. 1,4-dioxane).

Keywords: cycloaddition, Diels-Alder, 2,5-dimethylfuran, *p*-xylene, silica-alumina aerogels (SAA)

1. Introduction

The development of processes that convert biomass into fuels and chemicals are essential to reduce dependence on non-renewable resources such as fossil fuels [1, 2]. In this regard, research into the production of the commodity chemicals such as benzene, toluene, and xylenes from biomass has rapidly expanded in the past decade [3-5]. Especially, *p*-xylene is one major chemical of interest due to the increasing global consumption of terephthalic acid (TPA), used in the manufacture of plastic containers, synthetic fibers, and many other products [5-10].

A promising approach has recently been demonstrated for the production of renewable *p*-xylene. Williams et al. reported the one-pot conversion of biomass-derived 2,5-dimethylfuran (DMF) to *p*-xylene with good selectivity (~75%) through a Diels-Alder cycloaddition reaction over H-Y zeolite [11]. The conversion occurs in two-steps in which the first step is the Diels-Alder cycloaddition of DMF and ethylene to form an oxanorbornene cycloadduct intermediate and the second step is the dehydration of the resulting cycloadduct to *p*-xylene, as shown in Fig. 1. Competing side reactions such as the hydrolysis of DMF to 2,5-hexanedione (HDO) and the alkylation of *p*-xylene with ethylene can also occur and reduce *p*-xylene selectivity. Chang et al. recently showed that the addition of an aliphatic solvent, *n*-heptane, and the use of H-Beta zeolite further increase *p*-xylene selectivity to 90% by suppressing side reactions such as the formation of HDO [12]. Gas-phase DFT calculation showed that the Diels-Alder reaction of DMF and ethylene is thermally feasible (barrier of 24.7 kcal/mol), whereas the dehydration of the cycloadduct intermediate cannot proceed uncatalyzed (barrier of 58.0 kcal/mol) [13, 14]. The introduction of Brønsted acidic H-Y zeolite significantly lowered the dehydration barrier to 19 kcal/mol, indicating the necessity of a Brønsted acid catalyst. However, Brønsted acids did not show any potential for decrease

in the Diels-Alder reaction barrier, thereby making the uncatalyzed Diels-Alder reaction the rate-determining step for *p*-xylene production [12].

In addition to microporous zeolites, other types of solid acid catalysts have demonstrated high activity for the production of *p*-xylene. Wang et al. showed that good selectivity (~77%) to *p*-xylene can be achieved with amorphous WO_x-ZrO_2 and niobic acid due to its strong Brønsted acidity [15]. In a patented study, Brandvold reported that acid-washed activated carbon can produce *p*-xylene with 30% yield [16].

In this work, we investigate the Diels-Alder cycloaddition and subsequent dehydration of DMF and ethylene using silica alumina aerogel (SAA) catalysts. SAA demonstrates comparable activity for *p*-xylene production to H-Beta zeolite, which has been reported as the most active catalyst, under identical reaction conditions. A series of SAA catalysts with different Si/Al ratios were prepared and tested to study the effect of acid site density on the *p*-xylene production. We also examine the impact of solvent choice on the *p*-xylene yield using several polar and non-polar solvents.

2. Experimental

2.1. Catalyst preparation and characterization

H-ZSM-5 (SiO_2/Al_2O_3 = 30), H-Y (SiO_2/Al_2O_3 = 30), H-BEA-38 (SiO_2/Al_2O_3 = 38), and H-BEA-25 (SiO_2/Al_2O_3 = 25) were purchased from Zeolyst. SO_4-ZrO_2 (SZ) and WO_x-ZrO_2 were purchased from Alfa Aesar. SiO_2–Al_2O_3 (SA, SiO_2/Al_2O_3 = 11.2) was purchased from Sigma-Aldrich. Zirconium phosphate (Zr-P) was prepared by a co-precipitation method at a molar ratio of P/Zr = 2 as described elsewhere [17]. Acid-washed graphene oxide (GO) was prepared by impregnation of the graphene oxide with 60% phosphoric acid and followed by thermal activation at 1073 K. Silica-alumina aerogels (SAA) with different Si/Al ratios were prepared using a sol-gel method followed by CO_2 supercritical drying, based on the method

described elsewhere [18-21]. All the catalysts were calcined in a muffle furnace at 773-873 K for 4 h prior to reactions.

The compositions of the prepared aerogels were measured using inductively coupled plasma atomic emission spectroscopy (ICP-AES, Polyscan-61E). Based on the ICP-AES results, the silica-alumina aerogels containing Al/(Si+Al) = 0.12, 0.23, 0.33, 0.57, and 0.73 (mol/mol) were denoted as SAA-12, SAA-23, SAA-33, SAA-57, and SAA-73, respectively. In addition, alumina aerogel was denoted as AA. All the aerogel catalysts were further characterized by N_2-physisorption (BELSORP-mini II), NH_3-temperature programmed desorption (NH_3-TPD, BELCAT-B), and pyridine-Fourier transform infrared spectroscopy (pyridine-FT-IR, Jasco FT/IR-4100 spectrometer). Detailed procedures for the synthesis and characterization of the catalysts are given in the Supporting Information.

2.2. Catalytic experiments

Reactions were performed in a stainless steel 150 mL Parr reactor. DMF was reacted with catalysts at a loading of 0.15±0.05 g catalyst and 3.9 mL DMF (10 wt% initial concentration) in various solvents. Before reaction, the reactor was purged with N_2 and then pressurized to 20–30 bar with ethylene gas. The reactor was then heated up to 523 K and stirred at 300±50 rpm with a gas entrainment impeller. After reaction, liquid products were collected, filtered, and analyzed by using a gas chromatography equipped with flame ionization detector (GC-FID, Agilent 7890A). The products were identified and quantified based on the retention times and response factors of standard chemicals.

3. Results and Discussion

3.1. Effect of different acid catalysts

The Diels-Alder cycloaddition reaction of DMF and ethylene was studied with different types of acid catalysts at 523 K for 4 h. Fig. 2 shows the conversion of DMF, the selectivity to *p*-xylene, and the rate of *p*-xylene formation over several acid catalysts, and Table 1 summarizes the pore structure and acid sites of the catalysts as determined by N_2-physisorption and NH_3-TPD measurements, respectively. Among the tested zeolite catalysts, H-BEA-25 showed the highest conversion of DMF (55%) and the highest rate of *p*-xylene formation (9.63 mmol/g cat.h). H-ZSM-5 and H-Y zeolite had relatively low conversions of DMF (6.6 and 23.3%, respectively) and low rates of *p*-xylene formation (0.17 and 4.64 mmol/g cat.h). These results are consistent with prior work by Chang et al. [12], who reported that the reaction with H-BEA is more active than that with H-ZSM-5 and H-Y zeolite. Especially, the relatively low activity of H-ZSM-5 can be attributed to the slower diffusion of the reactants and products, such as DMF/ethylene cycloadduct, within the channels of H-ZSM-5 (5.5 - 5.6 Å) than within H-BEA-25 (6.6 - 6.7 Å) and H-Y (7.4 Å).

Compared to microporous zeolites, Zr-P, sulfated zirconia (SZ), WO_x-ZrO_2, and acid-washed graphene oxide (GO) all showed significantly low activity for the production of *p*-xylene. Although WO_x-ZrO_2 and acid-washed activated carbon showed high selectivity to *p*-xylene in previous studies [15, 16], very low selectivity to *p*-xylene (<30%) was observed with these catalysts here, possibly due to their low surface area or the absence of strong Brønsted acid sites. Amorphous silica alumina (SA) with Si/Al = 5.6 also exhibited low activity and low selectivity to *p*-xylene (<35%). Meanwhile, the silica alumina aerogel (SAA-57) showed remarkable selectivity to *p*-xylene (55%) and a high rate of *p*-xylene formation (9.81 mmol/g cat.h). The high activity of SAA-57 may be due to its high acid site density (1.16 mmol/g) and high surface area (411 m^2/g), which are comparable to those of H-BEA-25 as shown in Table 1. Importantly, SAA-57 has significantly larger pores which are 28 nm in

diameter and a higher total mesoporous volume of 1.207 cm^3/g compared to SA with pores 5.52 nm in diameter and a mesoporous volume of 0.473 cm^3/g.

Overall, H-BEA-25 and SAA-57 are the most active and selective catalysts for this reaction; they are able to convert DMF with more than 50% selectivity to *p*-xylene. At the higher conversion (X_{DMF} > 75%), SAA-57 was able to produce the higher yield of p-xylene than H-BEA-25.

3.2. Effect of the Si/Al ratio of silica-alumina aerogels (SAA)

Because SAA-57 showed the highest rate of *p*-xylene production among the tested solid acid catalysts, the aerogel catalysts were further investigated by varying the Si/Al ratio. Five SAA samples with different Al/(Si+Al) compositions (0.73, 0.57, 0.33, 0.23, and 0.12) were prepared for this purpose. N_2 adsorption measurements confirmed that all of the aerogel catalysts (except SAA-12) had high BET surface areas in the range of 351–473 m^2/g, large mesoporous volumes of 0.632–1.207 cm^3/g, and monodisperse mesopores of approximately 18.51–28.07 nm (see Table 1).

NH_3-TPD measurements revealed that the number of acid sites was proportional to the Al content of the SAAs. The total number of acid sites increased with an increase in Al/(Si+Al) in the following order: SAA-73 > SAA-57 > SAA-33 > SAA-23 ≈ SAA-12 (see Table 1). The FT-IR spectra after pyridine adsorption at 423 K were recorded to quantify the amount of Brønsted and Lewis acid sites as shown in Table 2. The amount of both Brønsted and Lewis acid sites increased as the mole fraction of Al for the SAAs was increased up to 0.57 and then decreased with a further increase in the Al mole fraction. However, the ratio of Brønsted to Lewis acid site density did not exhibit any correlation with the Al/(Si+Al) compositions of SAAs.

The conversion, product selectivity, and yield of *p*-xylene as a function of the bulk Si/Al ratio are shown in Fig. 3. The conversion of DMF and the yield of *p*-xylene increased with a decrease in the Si/Al ratio from 9 to 1 and then decreased with a further decrease in the Si/Al ratio. The highest conversion of DMF (90%) and the highest yield of *p*-xylene (60%) were obtained at Si/Al = 1. The alumina aerogel (AA) showed significantly low activity toward *p*-xylene production compared with the SAAs, indicating that Lewis acid sites are not effective at catalyzing the dehydration of the cycloadduct.

The conversion of DMF and the yield of *p*-xylene showed a close correlation with the concentrations of the Brønsted and Lewis acid sites over the SAAs. The yield of *p*-xylene increased linearly with the density of acid sites. It has been shown that the initial Diels-Alder reaction of DMF and ethylene proceeds uncatalyzed and the overall rate of *p*-xylene formation is controlled by the catalyzed dehydration of the cycloadduct for H-Y zeolite and WO_x-ZrO_2 [11, 13, 15, 22]. The rate of *p*-xylene formation increased with an increase in the concentration of Brønsted acid sites [22] . Thus, the variation of the yield of *p*-xylene with different Si/Al ratios of the SAAs can be explained by the dependence of the *p*-xylene production rate on the concentration of the Brønsted acid sites.

In addition to the effect of acid site concentrations, the change of the p-xylene yield over SAAs with different Si/Al ratios may be partially caused by the different deactivation performances of the SAAs because the deactivation of the catalysts occurred during the reaction by the formation of heavy oligomers on the catalyst surface (See Fig. S2). To check this possibility, the initial rates of p-xylene formation were measured over SAAs (See Fig. S4). The initial rate of p-xylene formation had linear dependence on the concentration of the Brønsted acid sites over the SAAs, suggesting that the contribution from the catalyst deactivation is insignificant.

For all of the aerogel catalysts, the selectivity to *p*-xylene was between 50–70%. The formation of several side products was also observed, as reported previously [11, 15]. These side products include HDO formed by the hydrolysis of DMF, 3-methyl-2-cyclopentenone (cyclopentenone) formed by the intramolecular aldol reaction of HDO, 1-methyl-4-propylbenzene (alkylated) formed by the alkylation of *p*-xylene with ethylene, 3,6-dimethyl-2-cyclohexen-1-one (cyclohexenone) formed by the isomerization of the DMF/ethylene cycloadduct, and oligomers formed by the secondary addition of DMF or ethylene (see Fig. 1).

3.3. Effect of different solvents

The Diels-Alder reaction of DMF and ethylene was carried out in different types of solvents, including heptane (non-polar), dioxane (polar aprotic), tetrahydrofuran (THF, polar aprotic), and isopropanol (IPA, polar protic) to investigate solvent effects, which may reduce the competing side reactions and increase the *p*-xylene selectivity. It has been shown that the use of heptane as a solvent greatly reduces side reactions such as the hydrolysis of DMF and the formation of oligomers from DMF [11, 23].

Fig. 4 shows the conversion of DMF, the product selectivity, and the yield of *p*-xylene in various solvents with SAA-57 and H-BEA-25 catalysts. For both catalysts, the conversion of DMF and the yield of *p*-xylene increased in the following order: IPA < heptane < THF < dioxane, whereas the *p*-xylene selectivity increased in the following order: IPA < heptane ≈ dioxane < THF, demonstrating an enhanced rate of *p*-xylene formation in polar aprotic solvents. Reactions in IPA, a polar protic solvent, exhibited the lowest *p*-xylene yields and high selectivity to HDO. This is attributed to the instability of IPA under the applied reaction conditions, where IPA is dehydrated to propene or 2-isopropoxypropane and releases water, thereby increasing the hydrolysis of DMF to HDO.

The higher *p*-xylene yields in the polar aprotic solvents, including dioxane and THF, compared to heptane may be due to either the enhanced Diels-Alder reaction rate or the enhanced dehydration reaction rate. It is well established that the Diels-Alder reaction rate increases when polar protic solvents such as water and ethylene glycol are used due to the hydrophobic packing and hydrogen bonding interaction [24-27]. However, the cases of polar aprotic solvents such as dioxane have rarely been reported. The direct measurement for the rates of cycloadduct formation in different solvents was not possible because the formation of the cycloadduct is not favorable thermodynamically at 523 K (ΔG_{rxn}= 2.28 kcal/mol), whereas the production of p-xylene is overwhelming favorable (ΔG_{rxn}= −38.56 kcal/mol) [11, 28]. Moreover, considering that the rate of *p*-xylene formation depends on the concentration of Brønsted acid sites, the overall rate is likely limited by the dehydration of the cycloadduct under the reaction conditions investigated. Therefore, compared to nonpolar solvents, the higher *p*-xylene yields in the polar aprotic solvents can be attributed to the enhanced dehydration rate.

To test this hypothesis, the rates of *p*-xylene formation at low conversion in different solvents were measured with H-BEA-25 at different solid acid concentrations, as described in Fig. 5. At a high solid acid concentration (7 mM), the rates of *p*-xylene formation in different solvents were similar to each other, indicating that the solvent effect is negligible when a sufficient number of Bronsted acid sites is available for the dehydration reaction and when the overall rate of *p*-xylene production is limited by the Diels-Alder reaction. On the other hand, at low solid acid concentrations (1.5 and 3 mM), the rates of *p*-xylene formation in dioxane and THF were higher than those in heptane, demonstrating an enhanced dehydration reaction rate in polar solvents. Also, this reactivity trend at low conversion suggests that the solvent effect is not caused by the change of deactivation performance due to the stronger extraction capability of oligomers from the catalyst surface. It is possible that the use of a

polar solvent stabilizes charged intermediates in the dehydration of the cycloadduct, thereby facilitating the dehydration reaction. Similar behavior was reported by Mellmer et al. and Weingarten et al. in their investigations of solvent effects for the dehydration of biomass-derived molecules [29, 30]. The use of polar aprotic solvents such as γ-valerolactone (GVL), THF, and dioxane has been shown to lead to significant increases in reaction rates and product selectivity for the dehydration of xylose and 1,2-propanediol, compared to water, due to the stabilization of the acidic proton and the protonated transition states [29]. Overall, these results demonstrate that the use of polar aprotic solvents accelerates the overall rate of *p*-xylene production by increasing the dehydration reaction rate.

4. Conclusions

In summary, amorphous silica alumina aerogel (SAA) is a highly active catalyst for the production of *p*-xylene from 2,5-dimethylene (DMF) and ethylene through a combination of Diels-Alder cycloaddition and dehydration reactions. The high activity of SAA can be attributed to its high surface area, large mesoporous volume, and high acid site concentrations. Over the SAA catalysts with different Si/Al ratios, the conversion of DMF and the yield of *p*-xylene are proportional to the concentration of the Brønsted acid sites, indicating that the overall rate of *p*-xylene production is limited by the dehydration of the cycloadduct of DMF and ethylene under the reaction conditions investigated. Among the tested SAAs, the highest *p*-xylene yield of 60% was obtained with the SAA with Si/Al = 1 (SAA-57). The solvent plays a significant role in enhancing the rate of *p*-xylene production. Polar solvents such as 1,4-dioxane lead to significant increases in the *p*-xylene production rate compared to heptane. This enhanced activity is likely due to the stabilization of charged intermediates in the dehydration of the cycloadduct, thereby facilitating the dehydration reaction.

Acknowledgements

This work was supported by the R&D Convergence Program of NST (National Research Council of Science & Technology) of Republic of Korea /Korea Institute of Science and Technology (KIST) (Project No. 2E25402). We acknowledge Dr. J. S. Yoon for providing the aerogel samples.

References

[1] G.W. Huber, S. Iborra, A. Corma, Synthesis of Transportation Fuels from Biomass: Chemistry, Catalysts, and Engineering, Chem. Rev., 106 (2006) 4044-4098.
[2] D.G. Vlachos, J.G. Chen, R.J. Gorte, G.W. Huber, M. Tsapatsis, Catalysis Center for Energy Innovation for Biomass Processing: Research Strategies and Goals, Catal. Lett., 140 (2010) 77-84.
[3] T.P. Vispute, H. Zhang, A. Sanna, R. Xiao, G.W. Huber, Renewable Chemical Commodity Feedstocks from Integrated Catalytic Processing of Pyrolysis Oils, Science, 330 (2010) 1222-1227.
[4] T.R. Carlson, Y.-T. Cheng, J. Jae, G.W. Huber, Production of green aromatics and olefins by catalytic fast pyrolysis of wood sawdust, Energy Environ. Sci., 4 (2011) 145-161.
[5] D.I. Collias, A.M. Harris, V. Nagpal, I.W. Cottrell, M.W. Schultheis, Biobased Terephthalic Acid Technologies: A Literature Review, Ind. Biotechnol., 10 (2014) 91-105.
[6] J.J. Pacheco, M.E. Davis, Synthesis of terephthalic acid via Diels-Alder reactions with ethylene and oxidized variants of 5-hydroxymethylfurfural, Proc. Natl. Acad. Sci. USA, (2014) 201408345.
[7] M. Shiramizu, F.D. Toste, On the Diels–Alder Approach to Solely Biomass-Derived Polyethylene Terephthalate (PET): Conversion of 2, 5-Dimethylfuran and Acrolein into p-Xylene, Chem. Eur. J., 17 (2011) 12452-12457.
[8] Y.-T. Cheng, Z. Wang, C.J. Gilbert, W. Fan, G.W. Huber, Production of p-Xylene from Biomass by Catalytic Fast Pyrolysis Using ZSM-5 Catalysts with Reduced Pore Openings, Angew. Chem. Int. Ed., 51 (2012) 11097-11100.
[9] Z. Lin, M. Ierapetritou, V. Nikolakis, Aromatics from Lignocellulosic Biomass: Economic Analysis of the Production of p-Xylene from 5-Hydroxymethylfurfural, AlChE J., 59 (2013) 2079-2087.
[10] Y. Tachibana, S. Kimura, K.I. Kasuya, Synthesis and Verification of Biobased Terephthalic Acid from Furfural, Sci. Rep., 5 (2015) 8249.

[11] C.L. Williams, C.-C. Chang, P. Do, N. Nikbin, S. Caratzoulas, D.G. Vlachos, R.F. Lobo, W. Fan, P.J. Dauenhauer, Cycloaddition of biomass-derived furans for catalytic production of renewable p-xylene, ACS Catal., 2 (2012) 935-939.
[12] C.-C. Chang, S.K. Green, C.L. Williams, P.J. Dauenhauer, W. Fan, Ultra-selective cycloaddition of dimethylfuran for renewable p-xylene with H-BEA, Green Chem., 16 (2014) 585-588.
[13] N. Nikbin, P.T. Do, S. Caratzoulas, R.F. Lobo, P.J. Dauenhauer, D.G. Vlachos, A DFT study of the acid-catalyzed conversion of 2, 5-dimethylfuran and ethylene to p-xylene, J. Catal., 297 (2013) 35-43.
[14] N. Nikbin, S. Feng, S. Caratzoulas, D.G. Vlachos, p-Xylene Formation by Dehydrative Aromatization of a Diels–Alder Product in Lewis and Brønsted Acidic Zeolites, J. Phys. Chem. C, 118 (2014) 24415-24424.
[15] D. Wang, C.M. Osmundsen, E. Taarning, J.A. Dumesic, Selective production of aromatics from alkylfurans over solid acid catalysts, ChemCatChem, 5 (2013) 2044-2050.
[16] T.A. Brandvold, Carbohydrate route to para-xylene and terephthalic acid, US 8314267 B2, 2012.
[17] N. Li, G.A. Tompsett, G.W. Huber, Renewable High-Octane Gasoline by Aqueous-Phase Hydrodeoxygenation of C5 and C6 Carbohydrates over Pt/Zirconium Phosphate Catalysts, ChemSusChem, 3 (2010) 1154-1157.
[18] J.S. Yoon, Y. Lee, J. Ryu, Y.-A. Kim, E.D. Park, J.-W. Choi, J.-M. Ha, D.J. Suh, H. Lee, Production of high carbon number hydrocarbon fuels from a lignin-derived α-O-4 phenolic dimer, benzyl phenyl ether, via isomerization of ether to alcohols on high-surface-area silica-alumina aerogel catalysts, Appl. Catal., B, 142 (2013) 668-676.
[19] W. Liu, A.-K. Herrmann, N.C. Bigall, P. Rodriguez, D. Wen, M. Oezaslan, T.J. Schmidt, N. Gaponik, A. Eychmüller, Noble Metal Aerogels—Synthesis, Characterization, and Application as Electrocatalysts, Acc. Chem. Res., 48 (2015) 154-162.
[20] N. Gaponik, A.-K. Herrmann, A. Eychmüller, Colloidal Nanocrystal-Based Gels and Aerogels: Material Aspects and Application Perspectives, J. Phys. Chem. Lett., 3 (2012) 8-17.
[21] N.C. Bigall, A.-K. Herrmann, M. Vogel, M. Rose, P. Simon, W. Carrillo-Cabrera, D. Dorfs, S. Kaskel, N. Gaponik, A. Eychmüller, Hydrogels and Aerogels from Noble Metal Nanoparticles, Angew. Chem. Int. Ed., 48 (2009) 9731-9734.
[22] R.E. Patet, N. Nikbin, C.L. Williams, S.K. Green, C.-C. Chang, W. Fan, S. Caratzoulas, P.J. Dauenhauer, D.G. Vlachos, Kinetic Regime Change in the Tandem Dehydrative Aromatization of Furan Diels–Alder Products, ACS Catal., 5 (2015) 2367-2375.
[23] R. Xiong, S.I. Sandler, D.G. Vlachos, P.J. Dauenhauer, Solvent-tuned hydrophobicity for faujasite-catalyzed cycloaddition of biomass-derived dimethylfuran for renewable p-xylene, Green Chem., 16 (2014) 4086-4091.
[24] D.C. Rideout, R. Breslow, Hydrophobic acceleration of Diels-Alder reactions, J. Am. Chem. Soc., 102 (1980) 7816-7817.
[25] R. Breslow, T. Guo, Diels-Alder reactions in nonaqueous polar solvents. Kinetic effects of chaotropic and antichaotropic agents and of .beta.-cyclodextrin, J. Am. Chem. Soc., 110 (1988) 5613-5617.

[26] J.F. Blake, W.L. Jorgensen, Solvent effects on a Diels-Alder reaction from computer simulations, J. Am. Chem. Soc., 113 (1991) 7430-7432.
[27] C. Chiappe, M. Malvaldi, C.S. Pomelli, The solvent effect on the Diels-Alder reaction in ionic liquids: multiparameter linear solvation energy relationships and theoretical analysis, Green Chem., 12 (2010) 1330-1339.
[28] Y.-P. Li, M. Head-Gordon, A.T. Bell, Computational Study of p-Xylene Synthesis from Ethylene and 2,5-Dimethylfuran Catalyzed by H-BEA, J. Phys. Chem. C, 118 (2014) 22090-22095.
[29] M.A. Mellmer, C. Sener, J.M.R. Gallo, J.S. Luterbacher, D.M. Alonso, J.A. Dumesic, Solvent Effects in Acid-Catalyzed Biomass Conversion Reactions, Angew. Chem. Int. Ed., 53 (2014) 11872-11875.
[30] R. Weingarten, A. Rodriguez-Beuerman, F. Cao, J.S. Luterbacher, D.M. Alonso, J.A. Dumesic, G.W. Huber, Selective Conversion of Cellulose to Hydroxymethylfurfural in Polar Aprotic Solvents, ChemCatChem, 6 (2014) 2229-2234.

Table 1. Pore structures and acid sites of the catalysts (Si2Al, SiAl, 7Si3Al, 8Si2Al, and 9SiAl are silica-alumina aerogels, whereas SiO_2-Al_2O_3 is a silica-alumina catalyst).

Catalyst	Si/Al ratio	Code	S_{BET} [a] (m^2g^{-1})	S_{micro} [b] (m^2g^{-1})	$S_{external}$ [c] (m^2g^{-1})	V_{pore} [d] (cm^3g^{-1})	V_{micro} [e] (cm^3g^{-1})	V_{meso} (cm^3g^{-1})	D_{meso} [f] (nm)	Acid sites ($mmol.g^{-1}$)
H-BEA-25	12.5	CP814E	545	367	178	0.493	0.269	0.225	9.36	1.12[12]
H-BEA-38	19	CP814C	574	475	99	0.342	0.282	0.060	3.77	1.21[12]
H-ZSM-5	15	CBV3024E	358	297	61	0.227	0.179	0.049	2.44	1.10[12]
H-Y	15	CBV720	739	634	105	0.473	0.363	0.110	4.27	0.58
$Zr(HPO_4)_2•H_2O$	N/A	Zr-P	77	10	67	0.117	0.033	0.084	3.77	0.78
WO_x-ZrO_2	N/A	WZ	88	6	82	0.231	0.038	0.193	10.70	0.74
SO_4-ZrO_2	N/A	SZ	162	46	116	0.231	0.072	0.159	8.19	1.23
SiO_2-Al_2O_3	5.6	SA	489	70	419	0.679	0.205	0.473	5.52	0.91
Si2Al	0.5	SAA-73	351	77	275	0.787	0.155	0.632	18.51	2.24
SiAl	1	SAA-57	411	68	343	1.387	0.180	1.207	28.07	1.16
7Si3Al	2.3	SAA-33	432	52	380	1.222	0.189	1.034	24.41	0.69
8Si2Al	4	SAA-23	473	87	386	0.905	0.208	0.698	24.41	0.60
9SiAl	9	SAA-12	189	39	150	0.259	0.084	0.175	3.77	0.63

[a] BET surface area

[b] Micropore area obtained by t-plot analysis

[c] External surface area obtained by t-plot analysis combined with BET surface area

[d] Single point adsorption total pore volume (P/P_0=0.99)

[e] Single point adsorption micro pore volume (P/P_0=0.20)

[f] Mean mesopore diameter obtained by BJH method

Table 2. Concentrations of the acid sites measured by pyridine-FT-IR.

Catalyst	Al/(Si+Al)	$\rho_{Brønsted}$ (μmol/g)	ρ_{Lewis} (μmol/g)	BA/LA
SAA-73	0.73	0.074	0.012	6.1
SAA-57	0.57	0.097	0.023	4.2
SAA-33	0.33	0.087	0.014	6.4
SAA-23	0.23	0.081	0.011	7.5
SAA-12	0.12	0.065	0.010	6.8

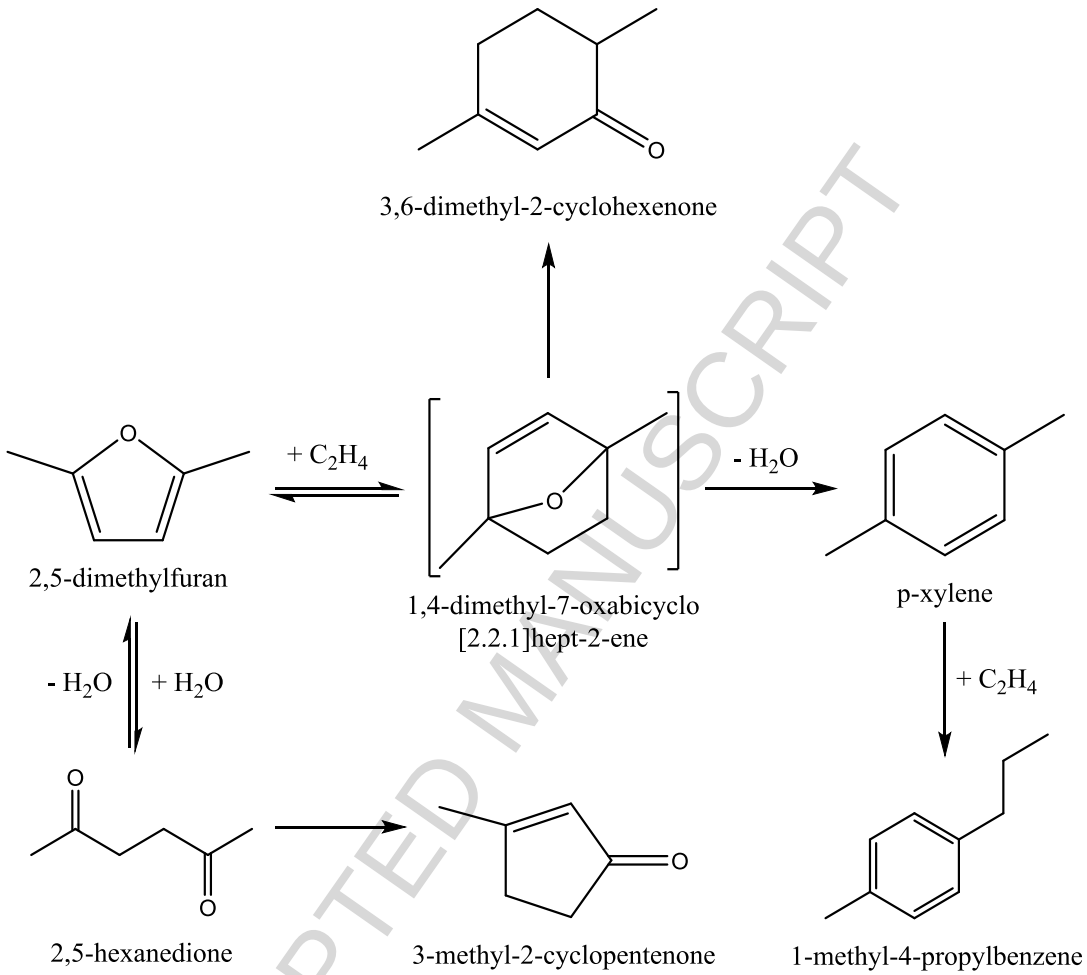

Fig. 1. Reaction pathway for the production of *p*-xylene via Diels-Alder cycloaddition between DMF and ethylene, and subsequent dehydration of an oxanorbornene cycloadduct [15].

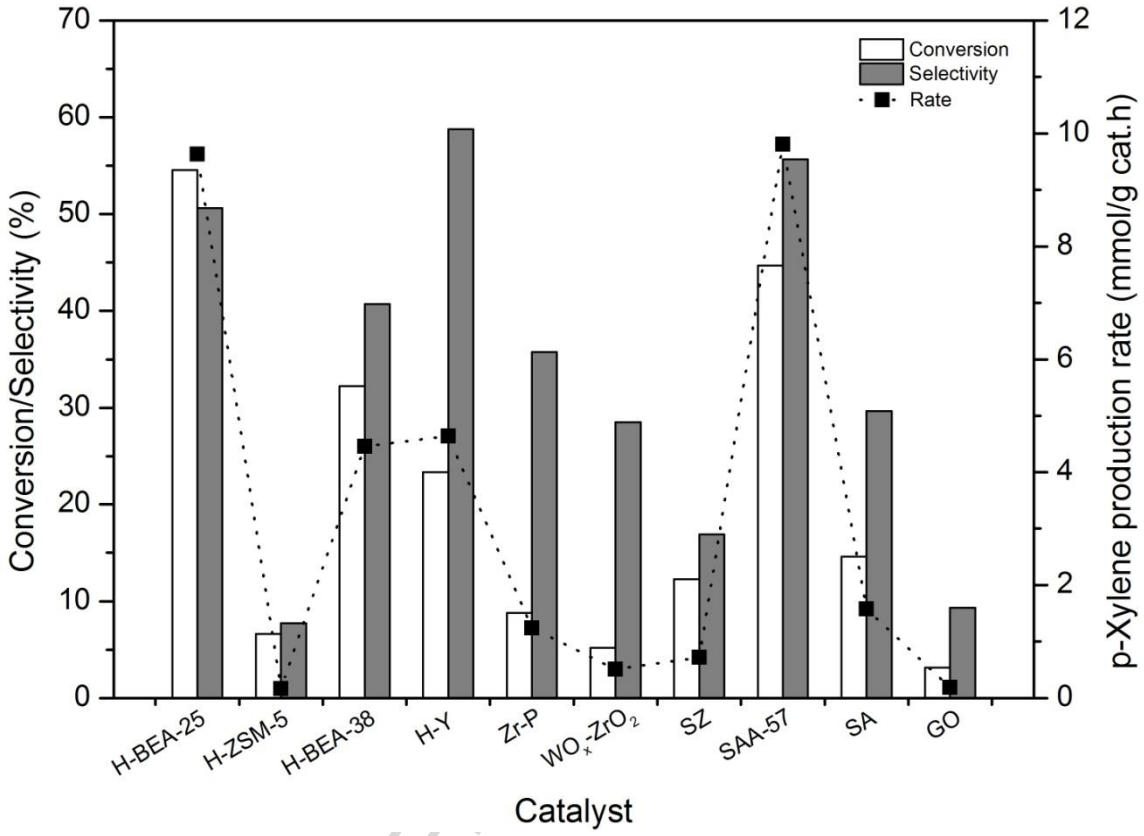

Fig. 2. Conversion, *p*-xylene selectivity, and rates of *p*-xylene formation in the Diels-Alder cycloaddition reaction of DMF and ethylene (20 bar) in heptane as a solvent at 523 K for 4 h with various catalysts.

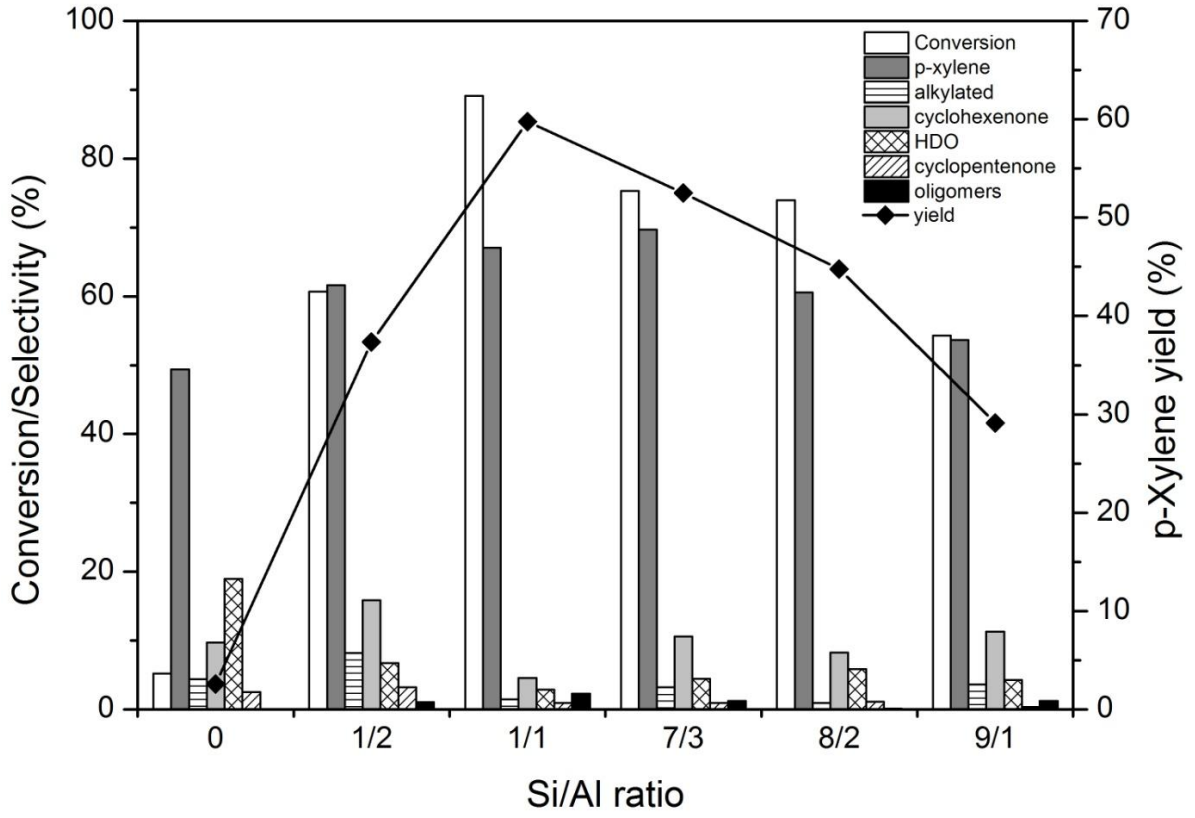

Fig. 3. Conversion and product selectivity for the reaction of DMF in dioxane with ethylene (30 bar) at 523 K for 6 h with SAAs with different Si/Al ratios.

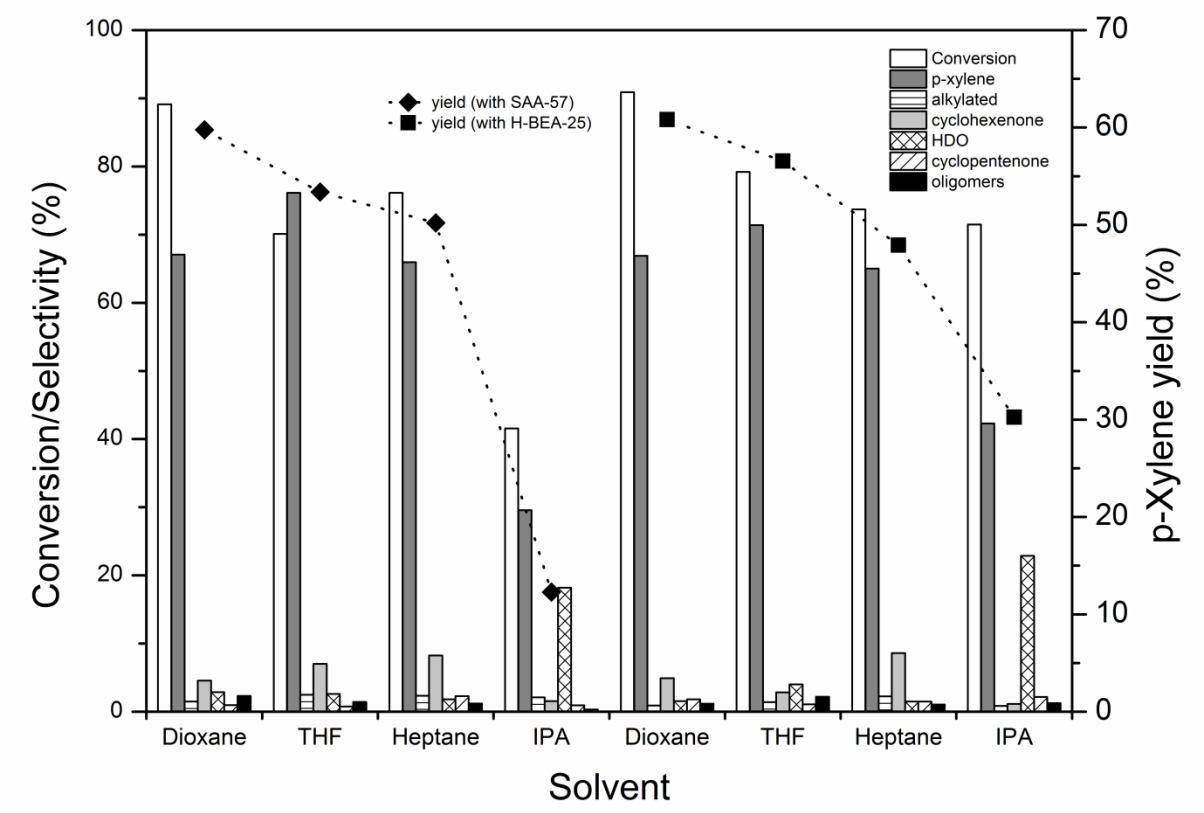

Fig. 4. Conversion and product selectivity for the reaction of DMF with ethylene (30 bar) at 523 K for 6 h in various solvents with SAA-57 and H-BEA-25.

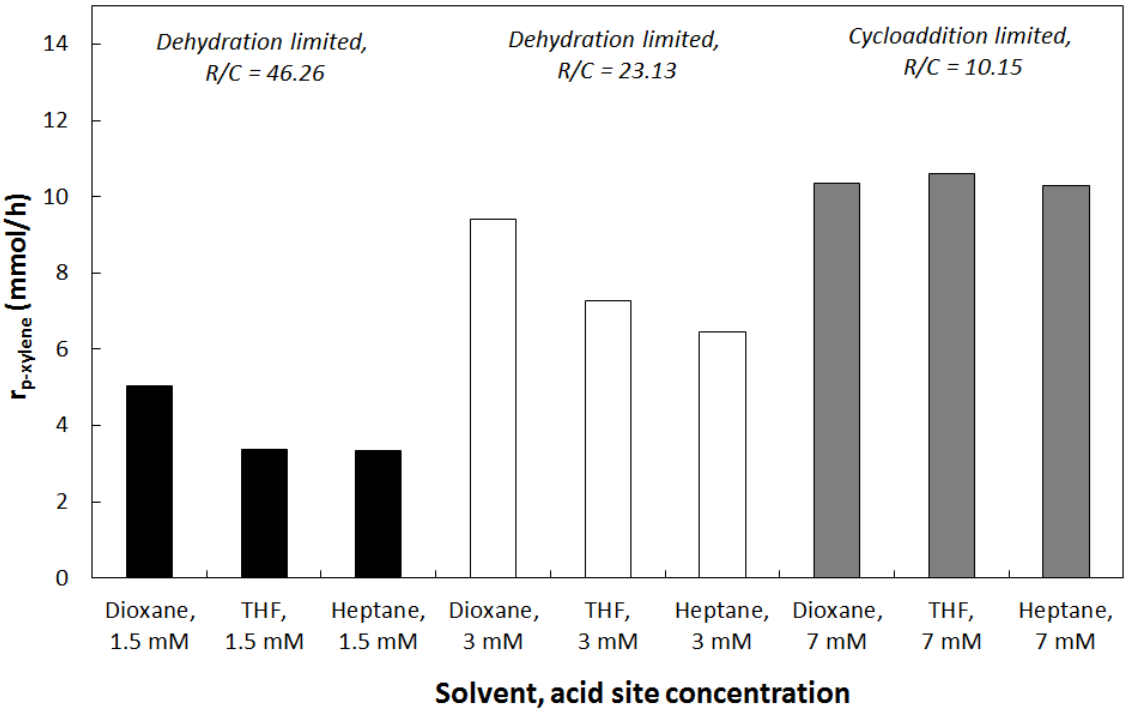

Fig. 5. Rate of *p*-xylene production with H-BEA-25 at 523 K at 1.5, 3, and 7 mM H-BEA acid site concentrations (R/C: reactant to catalyst mass ratio).

Highlights

- Cycloaddition of dimethylfuran for renewable *p*-xylene with silica alumina aerogels
- The *p*-xylene yield is a function of the concentrations of the Brønsted acid sites.
- The rate of *p*-xylene production increases significantly in polar aprotic solvents.